

Comparison of Josephson vortex flow transistors with different gate line configurations

J. Schuler,^{a)} S. Weiss, T. Bauch, A. Marx,^{a)} D. Koelle,^{b)} and R. Gross^{a)}

II. Physikalisches Institut, Universität zu Köln, Zùlpicher Str. 77, D - 50937 Köln, Germany

We performed numerical simulations and experiments on Josephson vortex flow transistors based on parallel arrays of $\text{YBa}_2\text{Cu}_3\text{O}_{7-\delta}$ grain boundary junctions with a cross gate-line allowing to operate the same devices in two different modes named Josephson fluxon transistor (JFT) and Josephson fluxon-antifluxon transistor (JFAT). The simulations yield a general expression for the current gain vs. number of junctions and normalized loop inductance and predict higher current gain for the JFAT. The experiments are in good agreement with simulations and show improved coupling between gate line and junctions for the JFAT as compared to the JFT.

The availability of a superconducting transistor is expected to significantly expand the application range of superconducting electronics. This has stimulated considerable activities towards the development of three-terminal devices based on Josephson junctions from high-transition-temperature superconductors (HTS), which offer high intrinsic speed due to large products of critical current times junction resistance. Among the various types which have been investigated, the Josephson vortex flow transistor (JVFT) shows probably the most promising performance [1]. In JVFTs the density of Josephson vortices in either a long Josephson junction or a parallel array of N small junctions is controlled by applying a magnetic field via a control (gate) current I_g flowing through a gate line. Hence, the critical current I_c or the voltage V across the junction(s), if biased at $I_b > I_c$, is controlled by I_g . A figure of merit is the current gain $g = |dI_c/dI_g|_{max}$, which is defined as the slope of the $I_c(I_g)$ characteristics in its steepest point. To maximize the current gain various JVFT designs have been developed which basically differ in (i) the *type of Josephson junctions*, i.e. either a single long junction or an array of N short junctions, coupled via $N-1$ loops (ii) the *junction geometry*, e.g. symmetric overlap or asymmetric in-line type and (iii) the *gate line geometry*, in particular the relative orientation of the gate line with respect to the junction(s).

We will focus here on parallel arrays of Josephson junctions which offer more flexibility in design parameters as compared to long junction JVFTs (e.g. variation of loop inductance L via the loop dimensions). In a standard geometry the gate line is positioned parallel to the array, as shown in Fig.1(a). We refer to this configuration as the *Josephson fluxon transistor (JFT)*. In this design the current gain can be drastically improved by introducing an asymmetric junction geometry [1,2]. Alternatively, instead of altering the bias current distribution, the gate line can be oriented perpendicularly to the junctions in the *Josephson fluxon-antifluxon transistor (JFAT)*, shown in Fig.1(b) [3,4]. The JFAT seems to show improved gain as compared to the symmetric JFT [3]. In this letter we present a comparative study of both designs by numerical simulation and by experiment, which is intended to clarify their different behavior

and which has not been understood so far.

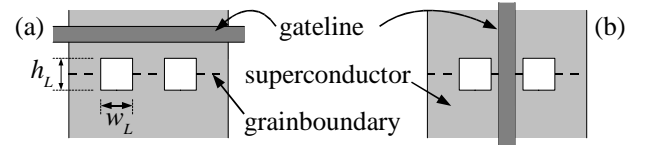


FIG. 1. Sketch of a JFT (a) and a JFAT (b) based on a discrete array of HTS grain boundary Josephson junctions.

To model both the JFT and JFAT we numerically calculated the $I_c(I_g)$ -characteristics for both gate line geometries by using the image current model [4] with an algorithm as described in detail in Ref. 5. In brief, the algorithm calculates the distribution of junction currents and transverse currents in a network of N parallel junctions coupled by $N-1$ loops as a function of applied magnetic flux and bias current distribution in a self consistent way. We use the first Josephson equation and fluxoid quantization for each Josephson junction and each loop and current conservation at each node of the array. Solutions for the maximum total supercurrent through the network I_c are obtained by an iteration method which is similar to the one developed for long junctions as described in [6]. The gate line is assumed to be separated from the bottom superconducting film by a thin insulating layer, and a gate current I_g induces an image current $I_i = -k_i I_g$ in the superconductor. Obviously, the gain scales linearly with the coupling constant $0 \leq k_i \leq 1$, and for the simulated $I_c(I_g)$ -characteristics we assume $k_i = 1$. All simulation results presented here were obtained with the assumption of homogeneous distributions of the bias current I_b , the critical junction currents I_c^0 and the inductance L of the loops with a fixed ratio $w_L/h_L = 2$ of loop width w_L and loop height h_L . To a first approximation the value of w_L/h_L does only affect the coupling coefficient. Hence, all results regarding the scaling of $g(N, \beta_L)$ are not affected by the choice of w_L/h_L .

^{a)}present address: Walther-Meißner-Institut, Bayerische Akademie der Wissenschaften, Walther-Meißner Str. 8, D-85748 Garching, Germany

^{b)}e-mail: koelle@ph2.uni-koeln.de

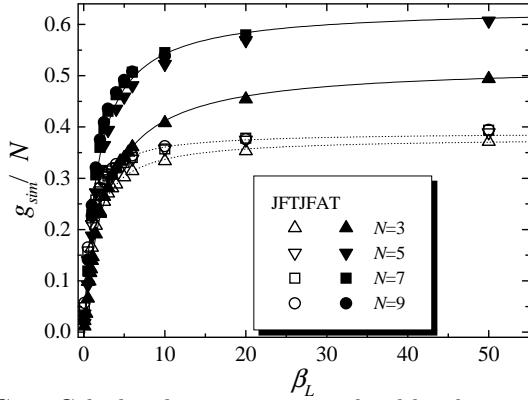


FIG. 2. Calculated gain g_{sim} normalized by the number of junctions N vs. normalized loop inductance β_L for a JFT and a JFAT. The lines are calculated from eq.(1).

From the numerically calculated $I_c(I_g)$ -characteristics we extract the current gain which depends on the type of gate configuration, number N of junctions in the array and on the normalized loop inductance $\beta_L = 2\pi L I_c^0 / \Phi_0$, where Φ_0 is the flux quantum. Figure 2 summarizes our simulation results in a plot of gain per junction g_{sim}/N vs. β_L for the JFT (open symbols) and the JFAT (solid symbols) for different values of N . For $N \geq 5$ the gain g_{sim} is linear in N for both gate line configurations. Only in the case of $N = 3$ the gains per junction are noticeably lower. Furthermore, g_{sim}/N increases monotonically with β_L and saturates at $g_{sim}/N = g_\infty$ if $\beta_L \gg \beta_0$. Finally, g_{sim}/N is higher for the JFAT than for the corresponding JFT, except for small values $\beta_L \leq 2.4$ (for $N = 3$) and $\beta_L \leq 0.6$ (for $N \geq 5$). In any case, $g_{sim}(N, \beta_L)$ can be very well fitted by

$$g_{sim} = N g_\infty \frac{\beta_L}{\beta_L + \beta_0}, \quad (1)$$

with the fit parameters g_∞ and β_0 given in table I.

To compare our numerical simulation results with the experiment we fabricated JVFTs based on $\text{YBa}_2\text{Cu}_3\text{O}_{7-\delta}$ (YBCO) grain boundary Josephson junctions. To place the gate line directly over the junction arrays we used a three layer process, with the YBCO film as the bottom layer separated by a polyimide insulating layer from the Au film forming the gate lines. The 100nm thick YBCO was epitaxially grown by pulsed laser deposition on a symmetric 24° SrTiO_3 bicrystal and subsequently patterned using standard photolithography and Ar ion beam milling. Then, the sample was spin coated with polyimide and after a soft-bake the polyimide was photolithographically patterned and post-baked. Finally, the top 50nm Au layer was deposited by e-beam evaporation using a lift off process to form the gate lines. All fabricated devices discussed in this paper have loop dimensions $w_L = 6\mu\text{m}$ and $h_L = 3\mu\text{m}$, and 1-2 μm wide junctions. Figure 3 shows a device with $N = 3$ junctions. Our design with a cross gate configuration permits two modes of operation either as a JFT or as a JFAT. This allows direct comparison of both transistor geometries within a *single device*.

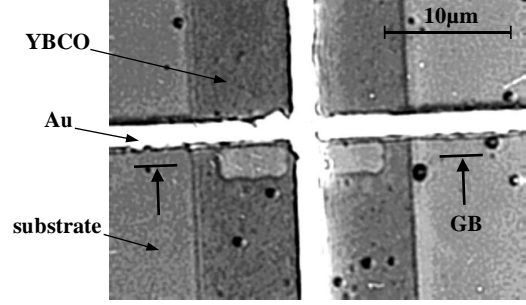


FIG. 3. Optical micrograph of a JVFT with $N = 3$ YBCO grain boundary junctions, and an Au cross gate line, which allows operation of the device either as JFT or as JFAT. The position of the grain boundary is marked as GB.

Figure 4 shows a direct comparison of the simulated and the measured $I_c(I_g)$ -characteristics of the device shown in Fig.3 in both modes of operation at 77.2K. We find reasonably good agreement of the simulated and the measured $I_c(I_g)$ characteristics, with $\beta_L = 13.4$ determined from the modulation depth of I_c [1,5]. Deviations are mainly caused by two aspects, which are not considered in the algorithm. Firstly, the critical current of the individual junctions is suppressed in a magnetic field, leading to reduced maximum I_c at the side maxima of the $I_c(I_g)$ -curves as compared to the maximum I_c at $I_g = 0$. Secondly, our algorithm does not include thermal fluctuations, which lead to a rounding of the measured $I_c(I_g)$ -characteristics.

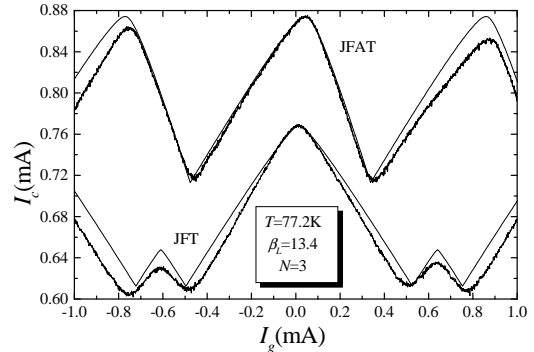


FIG. 4. Measured $I_c(I_g)$ -characteristics of a JVFT with $N=3$ operated as a JFAT and as a JFT. For comparison the calculated characteristics are shown as thin lines. For clarity the JFT-data are offset by $\Delta I_c = -0.1\text{mA}$.

Evidently, the experimentally realized gain of the JFAT ($g_{meas}^{JFAT} = 0.643$) is substantially higher than the gain realized in the JFT mode of operation ($g_{meas}^{JFT} = 0.386$), which can be attributed to two effects: Firstly, a smaller period $\Delta I_g = 4\pi I_c^0 (1 + \frac{h_L}{w_L}) / (k_i \beta_L)$ of the $I_c(I_g)$ -curves [1,5] for the JFAT increases its gain due to improved coupling to the gate line. From the measured ΔI_g and with $\beta_L = 13.4$ we determine $k_i = 0.488$ for the JFAT and $k_i = 0.326$ for the JFT. Secondly, an asymmetric distortion of the $I_c(I_g)$ characteristics of the JFAT increases its gain. This can be explained by considering the JFAT as a parallel connection of two asymmetric in-line type JFTs [1], with $(N - 1)/2$ loops [5]. This interpretation also explains the absence of

the small intermediate I_c -maxima for the 3-junction JFAT, which are present for the 3-junction JFT [cf. Fig.4].

Figure 5 shows a compilation of measured gains and coupling constants for different devices measured at variable temperature. We were able to achieve gains as high as 5.5 for a device with $N = 11$ junctions, which was operated as a JFAT. Here, only gains have been regarded, where the underlying $I_c(I_g)$ -characteristic does not show a discontinuity, as in such a point the gain cannot be defined at all.

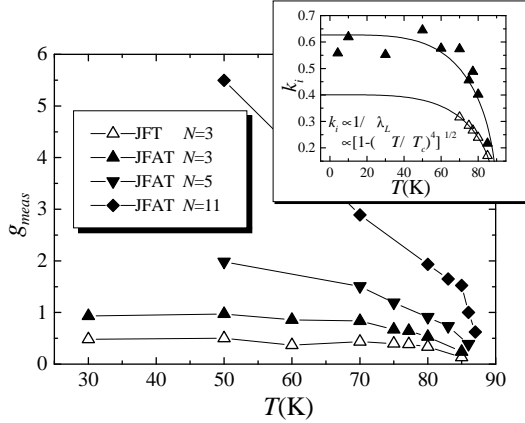


FIG. 5. Measured gain g_{meas} vs. temperature T for three devices. The inset shows measured (symbols) and fitted (lines) coupling constants $k_i(T)$ for the device with $N = 3$ junctions operated as JFT and JFAT.

We note that g increases with decreasing T for two reasons: Firstly, we expect from our simulations that g increases with β_L , which becomes larger by lowering T due to increasing I_c^0 . Secondly, the gain increases linearly with k_i , which is expected to approximately scale as $1/\lambda_L$ [5], in fairly good agreement with the data shown in the inset of Fig.5. To compare the experimental data with the simulation results shown in Fig.2 we normalize the measured gain by the number N of junctions and by the fitted $k_i(T)$ and plot it vs. β_L as determined from the modulation depth of I_c . The result is shown in Fig.6 for the device shown in Fig.3 with $N = 3$.

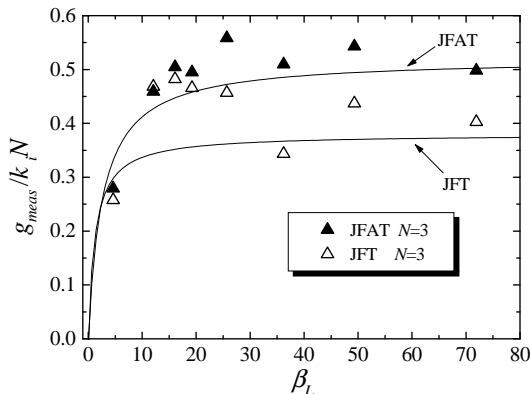


FIG. 6. Measured normalized gain $g_{meas}/(k_i N)$ vs. β_L for a device with $N = 3$ junctions operated as JFT and JFAT. The lines show the theoretical prediction from eq.(1) based on numerical simulations.

We find reasonable agreement between the experimental data and the theoretical lines, which are plotted from eq.(1) with the values for the fitting parameters from table I. The significant scatter of the data points is not surprising, given the scatter in the data of $k_i(T)$ for the JFAT and the uncertainty in $k_i(T)$ for the JFT for $T < 70$ K [cf. inset of Fig.5]. The most significant deviation from the numerical simulation is found for the JFT-data which lie significantly above the theoretical result for $10 < \beta_L < 25$. The reason for this deviation has not been clarified yet.

In conclusion, our numerical simulations of the $I_c(I_g)$ -characteristics of JVFTs based on a parallel array of junctions with two different gate line configurations predict superior behavior of the JFAT over the JFT with respect to current gain. Our experiments on JVFTs from YBCO Josephson junctions with cross gate geometry allow direct comparison of both types of JVFTs which resulted in an experimental confirmation of the numerical simulation results. The reason for the superior behavior of the JFAT is twofold: (i) the JFAT can be viewed as two parallel JFTs with asymmetric inline junction geometry which induces asymmetric $I_c(I_g)$ -characteristics and, hence, an increase in current gain over the symmetric JFT, and (ii) the coupling between gate line and the junction array is almost a factor of two higher in the JFAT configuration. The latter effect is not included in the simulation results, but has been shown experimentally.

-
- [1] R. Gross, R. Gerdemann, L. Alff, T. Bauch, A. Beck, O. M. Froehlich, D. Koelle, A. Marx, Appl. Supercond. **3**, 443 (1995).
 - [2] R. Gerdemann, T. Bauch, O.M. Froehlich, L. Alff, A. Beck, D. Koelle, R. Gross, Appl. Phys. Lett. **67**, 1010 (1995).
 - [3] S.J. Berkowitz, Y.M. Zhang, W.H. Mallison, K. Char, E. Terzioglu, M.R. Beasley, Appl. Phys. Lett. **69**, 3257 (1996).
 - [4] E. Terzioglu, M.R. Beasley, Y.M. Zhang, S.J. Berkowitz, J. Appl. Phys. **80**, 5483 (1996).
 - [5] Jürgen Schuler, Diploma Thesis, Universität zu Köln (1998).
 - [6] B. Mayer, H. Schulze, G.M. Fischer, R. Gross, Phys. Rev. B **52**, 7727 (1995).

TABLE I. Fit parameters obtained by fitting the simulation results to eq.1.

Type	N	g_∞	β_0
JFT	3	0.380	1.27
	≥ 5	0.390	0.80
JFAT	3	0.521	2.64
	≥ 5	0.632	1.67